Lyocell Fibre Production Using NMMO – A Simulation-based Techno-Economic Analysis

Eemeli Hytönen,[a,]* Lotta Sorsamäki,[b] Erik Kolehmainen,[a] Michael Sturm,[c] and Niklas von Weymarn [a]

The demand for man-made cellulosic fibres is expected to grow in the future. One commercially-available concept to supply fibres is Lyocell manufacturing from dissolving wood pulps using N-Methylmorpholine N-oxide (NMMO) as the solvent. The literature qualitatively indicates that NMMO recycling efficiency is a key factor for profitable operation. Process design information and parameter data are however poorly available publicly to illustrate the cost factors. Therefore, systematic techno-economic analysis of a 50 kt/year Lyocell plant was conducted using steady-state process simulation and cost modeling. With the simulation models, the underlying technical process design and modelling decisions, and economic assumptions were studied. NMMO makeup need is an important cost item. The simulated makeup need is very dependent on the design of the solvent recovery system and the vapor-liquid equilibrium thermodynamic model selection. On the other hand, water use, fibre washing process design, and washing model parameterization have relatively lower impact on the cost of production. Raw material cost and capital expenses are most critical cost items when the NMMO recycling efficiency is high.

DOI: 10.15376/biores.18.3.6384-6411

Keywords: Lyocell; Textile fibre; NMMO; Modelling; Process simulation; Feasibility; Thermodynamic model

Contact information: a: Metsä Spring Oy, Revontulenpuisto 2 A, 02100 Espoo, Finland; b: VTT Technical Research Centre of Finland Ltd., P.O. Box 1603, 40101 Jyväskylä, Finland; c: Thüringisches Institut für Textil- und Kunststoff-Forschung Rudolstadt e. V., Breitscheidstraße 97, 07407 Rudolstadt, Germany;
** Corresponding author: eemeli.hytonen@metsagroup.com*

INTRODUCTION

The process for producing Lyocell fibres from dissolving grade pulps using N-Methylmorpholine N-oxide (NMMO) as solvent is by now well developed. The development history of the amine oxide technology, called in this work NMMO-Lyocell process, until year 1999, has been reviewed *e.g.* by Perepelkin (2007) and White (2001). Several commercial NMMO-Lyocell production plants have been erected around the world during the last thirty years. In the 1990s, there were simultaneous developments in different countries. Courtaulds Fibres started three Tencel® plants, the first two in the USA and the third in the UK (Courtaulds part of Acordis) with original capacities of 16, 20, and 20 kt/a. Also, Lenzing built their first NMMO-Lyocell plant with capacity of 12 kt/a in Austria. Since then, Lenzing has expanded their production in Austria and acquired the plants originally operated by Courtaulds Fibres. It has quite recently also constructed a 100 kt/a plant in Thailand, which was started up in 2022. Recently, also other players in Asia and Turkey have initiated production and sales of Lyocell fibres. In search for sustainable alternatives for responding to the increasing need of textile fibres, other technologies using NMMO or other cellulose solvents have been developed (Golova *et al.* 2000; Sayyed *et al.* 2019; Makarov *et al.* 2020). In addition, modifications to the two slightly differing original NMMO processes by Courtaulds Fibres and Lenzing have been proposed (Wendler *et al.* 2012; Lidhure *et al.* 2019).

The NMMO-Lyocell process consists of two principal elements, the fibreline and the NMMO recovery. The first element is described in detail, *e.g.* in (White 2001), and the latter by Guo *et al.* (2021). From a plant design perspective, in addition to understanding the basic functions of the process elements, such as making dope, washing the fibre, or evaporating excess water from the dilute solvent, it is crucial to capture the reactions and phase changes of key process compounds. These phenomena have been studied experimentally: degradation and regeneration of NMMO (Rosenau *et al.* 2001), NMMO/H_2O and NMMO/H_2O /cellulose systems phase behavior under varying process conditions (temperature, pressure, composition) (Biganska and Navard 2003, 2004; Eckelt *et al.* 2009), and separation efficiencies of system compounds in fibreline functions, *i.e.* the mass transfer of key compounds (Hedlund *et al.* 2019). Further understanding on the phenomena is available outside the NMMO-Lyocell fibre production context. A noticeable body of scientific work has been created in the last 10 years in lignocellulosic biomass pre-treatment using NMMO. This has been summarized by Satari *et al.* (2019).

Systematic techno-economic analysis using process simulation and cost modelling plays an important role in assessment of process concepts and hence, in steering the development work. Using such bottom-up approach supports identification of the impacts of differences in scope and underlying assumptions related to the technology and economics of the considered concepts. Such analysis always encompasses several models that are used iteratively, and suitable modelling techniques and methods need to be selected carefully for each design stage. The goals and important limitations to be considered in an overall techno-economic assessment in different design stages are reviewed, *e.g.*, by Hytönen and Stuart (2013) and Towler and Sinnott (2008). In any techno-economic study based on process simulation, capabilities of different methods for modelling of thermodynamics, physical properties, kinetics, individual process equipment, and process integration need to be evaluated and suitable methods selected. Moreover, in the economic assessment also the method for evaluating fixed costs and specifically for estimation of capital costs recalls consideration. A good analysis and guide for selection of capital cost estimation routine was published by Tsagkari *et al.* (2016). A key guiding principle, in selection of the models, is to assess first relevance of all models in the case and the availability of required input data for all considered concepts.

Very few studies present systematic process simulation of a Lyocell process, or economic assessment of processes using NMMO as the solvent. Bouwman (2008) used a computational fluid dynamics (CFD) approach to study certain process equipment in the fibreline of the Lyocell process. Shao *et al.* (2003) constructed a mathematical model of the spinning process to specifically simulate NMMO diffusion coefficient inside the fibre. In some studies, mathematical models have been used to describe certain phenomenon, such as NMMO/H_2O system thermodynamics (Eckelt *et al.* 2009; Eckelt and Wolf 2008). The only plant-wide model of the complete process, reported in the literature to date, was developed by Reipsar (2020). He described the Lyocell process, and a model was used to simulate this process for studying different solvent recycling techniques. Modelling at a level higher than process modelling has been presented by Shen and Patel (2010). However, such models of the life cycle or supply chain are not commonly useful for process design, because they do not contain the process behavior in high detail. Specifically, no techno-economic assessments of Lyocell fibre production process have been published before. Only a few plant-wide process simulation -based process optimization studies of other fibre production processes have been reported (Bialik *et al.* 2020). Other context utilising NMMO as a lignocellulosic material pre-treatment solvent for production of ethanol or biogas from forest residues, pine or spruce, and food industry side-streams has been examined using process techno-economic analysis (Shafiei *et al.* 2011, 2014; Teghammar *et al.* 2014; Oliva *et al.* 2022).

In summary, based on the available literature, usable information for engineering process design and design analyses of Lyocell production process is very limited or non-existent. For example, overall techno-economic analysis studies of Lyocell processes are not publicly available. Furthermore, some papers discuss that fibre washing and NMMO recycling using evaporation are important costs defining process sections, but the needed process design parameter data and cost data are not available for verifying these claims. Therefore, the main goal of this work was to study the implications of the efficiency of evaporation and washing on the techno-economics of the NMMO-Lyocell production process. Process design and description of a feasible NMMO-Lyocell production plant, and a process simulation model and a cost model of this design, were developed to study these implications systematically. In the following chapters, the method, process design and models, and the analyses are described.

EXPERIMENTAL

Overall Methodology

The overall method of the study is a steady-state simulation model-based techno-economic analysis. The used method is suitable for conceptual and pre-feasibility-level engineering analyses. In such analyses, the target process design and key design parameters are obtained from literature and other available sources, such as experimental work, expert opinion, or past projects if available. The design is then modelled using a simulation software to obtain the mass and energy balances. The models are used to describe key technical features and are the basis for economic analysis. In case when sufficient design and design parameter data are not available, engineering design knowhow is used to compile the needed data set to construct the models. Furthermore, developing the process design iteratively using process simulation, model parameter estimation can be conducted simultaneously.

The economic analysis combines price and cost data with the balance data to get variable production cost estimates in EUR/t. Capital cost estimates are obtained using methods suitable for concept screening or feasibility study (Christensen and Dysert 2005), and factorial methods are used to get fixed production cost estimates. Combining these, production costs can be obtained.

The next chapters describe in more detail the overall method used in this work. First, the hypothetical case study and the evaluated scenarios are described. Then the development of the process simulation model including the modelling of thermodynamics and fibre washing, as well as the approach for electricity consumption calculation are explained. Finally, the approach for conducting the economic analysis is presented.

Case Study

The scope of the hypothetical case study covers the fibreline of the Lyocell process (incl. pre-treatment, dissolution, fibre spinning, washing, and drying process steps) and the NMMO recovery and recycling process (incl. flotation/filtration, ion-exchange, evaporation, and NMMO regeneration process steps). Figure 1 presents the block-flow diagram of the process with all inputs and outputs. The process flowsheet is defined based on publicly available information, *e.g.* (White 2001; Zauner 2017; Jiang *et al.* 2020). The production of utilities (air, chemicals, cooling water, fresh water, and steam) and wastewater treatment are not included in the scope of the study. Instead, utilities are assumed to be available at the site, and they are considered in the economic analysis through cost contributions.

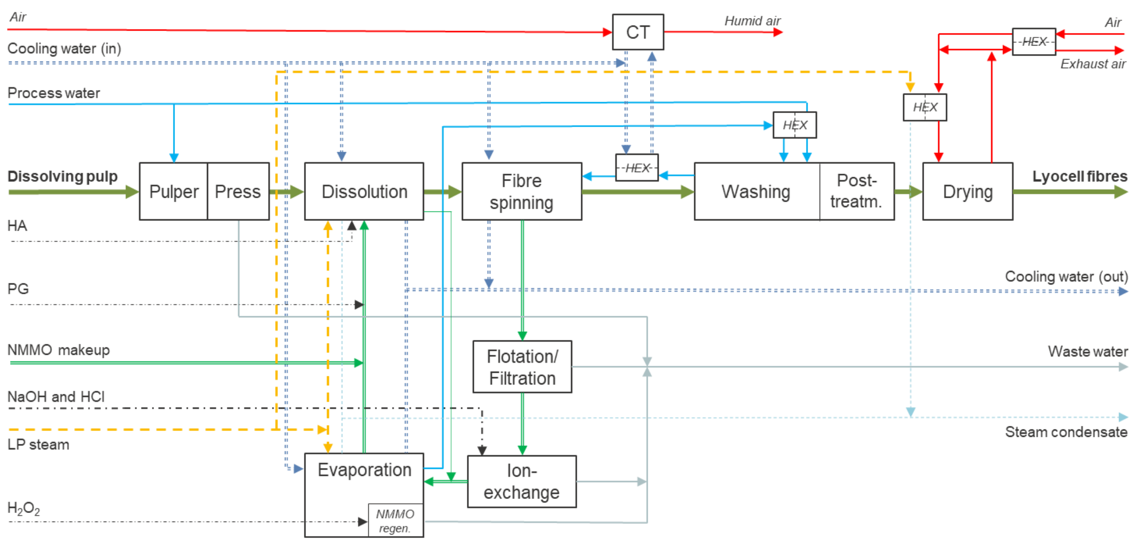

Fig. 1. Block-flow diagram of NMMO-Lyocell process. Abbreviations: CT = cooling tower, HEX = heat exchanger, NaOH = sodium hydroxide, HCl = hydrochloric acid, PG = propyl gallate, HA = Hydroxylamine, H_2O_2 = hydrogen peroxide, LP = low pressure. Line styles: solid olive green = fibre, double compound green = NMMO, dash-dot black = chemicals, dash yellow = LP steam, dash blue = steam condensate, solid light blue = process water, double compound-dash ice-blue = cooling water, solid red = air, solid grey = wastewater

In the pre-treatment block (pulper/press in Fig. 1), dry dissolving pulp is activated in a pulper by mixing with fresh (de-ionized) water. Sulfuric acid and sodium hydroxide can be used for pH-control. The activated pulp is pressed to as high dry matter as possible. In the dissolution block, the dewatered pulp is then mixed with recycled and makeup NMMO to form pre-dope. The pre-dope is mixed well in a ploughshare mixer, and water is evaporated under vacuum in a thin film evaporator to dissolve cellulose and form dope. Vacuum is used to prevent the degradation of NMMO solution which occurs if the solution is overheated. The evaporated vapors from dissolution are condensed and sent to NMMO recycling (evaporation block) to recover any evaporated NMMO. The dope is led to the fibre spinning block where it is drawn into a spinning bath. The bath is kept in constant temperature using cooling water, and in constant NMMO concentration by controlling the washing waters entering the bath. The bath receives continuously water from the washing block and the corresponding amount of bath liquid is led to NMMO recycling process. The formed fibre is led to a five-step counter-current washing block. Fresh water is used in the 5th washing step and recycled process water from solvent evaporation is fed to 4th washing step. The excess washing filtrate from each step is led to previous step and finally to spinning bath. Washing water amount is set to obtain the target residual NMMO content in the fibre, and to supply enough water to spinning bath to obtain the target NMMO content of the bath. The fibre is treated (finishing, cutting, bleaching) to targeted properties in post-treatment block. Washing water going to spinning bath is cooled using a cooling tower to reduce the need for cooling water. The washed and post-treated fibre is dried in the drying block using warm air. The drying air is circulated and mixed with fresh air before heating using low pressure steam. Circulation is controlled by adjusting air moisture close to dew point. Heat is further recovered from the exhaust air using heat exchanger.

The NMMO recovery process starts with flotation/filtration block, where solids and dissolved compounds are removed from the spent NMMO solvent. The partially cleaned solvent is then led to ion-exchange block where charged compounds are removed from the solvent. The anion and cation exchange columns are regenerated with sodium hydroxide and acid wash when their absorption capacity is reduced. The cleaned solvent is led to a six-stage co-current evaporation system. Pressure is decreased in the evaporators towards the last stage to keep the evaporation temperature in target range. Evaporation vents and the evaporated water from the last stage are collected, condensed, and fed back to the evaporation system. Water evaporated in three first stages is collected and recycled to fibre washing, whereas water evaporated in the 4^{th} and 5^{th} stage is recycled back to the evaporation system. NMMO-monohydrate is recovered from the last evaporation stage. NMMO degradation and regeneration is handled in the evaporation block, where the major part of the degradation product NMM (N-Methylmorpholine) is regenerated with hydrogen peroxide (H_2O_2) back to NMMO. Finally, the recovered NMMO-monohydrate is mixed with fresh NMMO-monohydrate makeup. Propyl gallate is added to reduce NMMO degradation. Hydroxylamine is also used to reduce fibre degradation.

The process design specifications for the considered NMMO-Lyocell plant are shown in Table 1. Even though several NMMO-Lyocell plants are commercially operating globally and thus the technology readiness level (TRL) is 9, actual plant and plant design data were not available for this study. Instead, all parameters are based on information available in the literature or expert opinions

Table 1. Key Process Design Specifications of the Considered NMMO-Lyocell Plant

Plant Capacity		Annual Production Capacity	50	kt/a, 88.9% Dry Matter
		Plant availability	95	%
NMMO Recovery Rate			99.7	%
Pre-Treatment	Dissolving pulp composition [a]	Dry content	92	%
		Cellulose	96.3	% on dry matter
		Hemicelluloses (C5 & C6)	3.55	% on dry matter
		Lignin	0.05	% on dry matter
		Inorganics	0.1	% on dry matter
		Pulper consistency	5	%
		Dry content after pre-treatment	50	%
		Pulp losses	0.5	% on dry matter
Dissolving		Temperature (max)	105	ºC

	Dope composition	Pulp based organic compounds (cellulose, hemicelluloses, lignin)	12.5	%
		Solvent	75.25	%
		Water	12.25	%
		Dissolving yield	100	%
Fibre Spinning		Bath temperature	20	ºC
		Spinning yield	100	%
		Bath NMMO content	20	%
		Bath consistency	0.5	%
Washing		Solvent content of fibre after washing	< 0.1	% on dry pulp
Drying		Final fibre dry content	88.9	%
		Drying air temperature	max. 120	ºC
		Moisture of leaving drying air	100	g/m3
		Fresh air temperature	18	ºC
Solvent Recovery		Filtration NMMO loss	0.01	%
	Ion exchange (Anion and cation exchange column)	Flow through rate	3	BV/h
		Column regeneration solution concentration	5%	NaOH and HCl
		Column regeneration solution dose	1.5	Times resin volume
		Running time	24	h
		Make-up NMMO	50	m-% NMMO content
		Recovered NMMO temperature	88	ºC
		Evaporator heat losses	2	%
		Evaporator vent fraction	0.5	%
	Boiling point elevation	50:50 NMMO:H_2O	8	ºC
		86:14 NMMO:H_2O	45	ºC
		NMMO concentration after recovery	86	%
	Share of degraded NMMO [b]	NMM	75	% of degraded
		non-recoverable compounds	25	% of degraded
		H_2O_2 dose	1	% excess over stoichiometric need
		Propyl gallate (PG) dose	0.2	m-% on cellulose
		Hydroxylamine (HA) dose	0.1	m-% on cellulose
Utilities		Cooling water temperature	15	ºC
		Fresh water temperature	15	ºC
		Cooling tower relative exit air humidity	100	%
		Cooling tower ambient air temperature	18	ºC
		Steam temperature	150	ºC
		Steam pressure	450	kPa

[a] Sixta 2006, [b] Kalt *et al.* 1999

Evaluated Scenarios

Four different scenarios were defined to study the implications of key process design specifications and modelling decisions. The scenarios are described in Table 2. To be able to draw distinct conclusions from the scenario comparisons, as many process design specifications as possible were kept constant.

The Base-case scenario describes the baseline of the process. The target of the Simplified recovery scenario is to reveal how the simplification of the NMMO recovery process (three-stage evaporation system and exclusion of NMMO regeneration) affects the economics. In Ideal thermodynamics scenario, the effect of the VLE model selection on the resulting economics is studied. The UNIFAC (universal functional activity coefficient) VLE model considers the molecular associations (interactions) between water and NMMO whereas Raoult's law considers all compounds as individuals without any interactions. In the fourth scenario, the effect of reduced NMMO content in the spinning bath on the economics was in focus.

Table 2. Scenario Definitions

Scenario	Base Case	Simplified Recovery	Ideal Thermodynamics	Low NMMO Content in Spinning Bath
Spinning bath NMMO content	20%	20%	20%	15%
Evaporation	6 step	3 step	6 step	6 step
Degraded NMMO recovery	yes	no	yes	yes
VLE model	UNIFAC	UNIFAC	Raoult's Law	UNIFAC
NMMO/H_2O solution	Non-ideal	Non-ideal	Ideal	Non-ideal

To enable transparent comparison, in the Ideal thermodynamics scenario three process design settings were adjusted: 1) the temperatures after evaporative process steps (dissolution, multi-effect evaporation in NMMO recovery) were set to the Base-case -scenario values by adjusting pressure profiles in evaporation, 2) water recycling rate was adjusted to reach the target fibre NMMO content, and 3) relative NMMO degradation was kept the same instead of targeting fixed NMMO recycling rate.

Process Simulation Model

Mass and energy balance model

For obtaining the mass and energy balances of the NMMO-Lyocell process, a steady-state simulation model is used. The process simulation model was developed using commercial steady-state simulation software Balas (Espoo, Finland).

The model topology is developed using MS Visio and the model is parametrized using the user interface of the software. The topology consists of units and streams; the streams transfer material information between the units that represent actual process equipment. The streams are in thermodynamic equilibrium in the conditions they leave their unit of origin, and they represent the process streams using three phases – solid, liquid and vapor.

Model compounds needed in the modelling of the NMMO-Lyocell process, and the phases they can exist in the model, are listed in Table 3. The thermodynamic properties of the solid-liquid model compounds are from Paccot (1987), and the properties of the liquid-vapor compounds are from Reid *et al.* (1977). The model compound named NMMO is a composite compound for all forms of NMMO in the system.

This simplification is needed to avoid managing many different model compounds in the model. The process is parametrized in such a way that the streams containing this compound are in molten state (the NMMO/H_2O ratio and temperature above phase diagram line (Biganska and Navard 2003)).

Table 3. Model Compounds and Their Possible Phases in the Modelling Environment

	Model Compound	Solid	Liquid/Dissolved	Vapor
Pulp	Cellulose	x	x	
	Lignin	x	x	
	Hemicellulose (C5)	x	x	
	Hemicellulose (C6)	x	x	
	Inorganics	x	x	
Water	H_2O		x	x
Chemicals	NaOH		x	
	HCl		x	
	H_2O_2		x	
	NMMO		x	x
	NMM		x	x
	Morpholine (C_4H_9NO)		x	x
	Formaldehyde (CH_2O)		x	x
	Propyl gallate (PG)	x	x	
	Hydroxylamine (HA)		x	x
Gases	Oxygen		x	x
	Nitrogen		x	x
	Carbon dioxide		x	x

User specified reactions, in addition to phase changes solved automatically by the simulator, are the dissolution of pulp-based compounds in dissolution block and the regeneration of dissolved compounds in the fibre spinning block. It is assumed that all pulp-based compounds dissolve completely, and no degradation of carbohydrate polymers to monomers occur. It is also assumed that 100% of dissolved pulp-based compounds will regenerate.

NMMO losses in the process are partly result of decomposition of NMMO to NMM and further to morpholine and formaldehyde. The major part of the degradation product (NMM) is regenerated with H_2O_2 back to NMMO (Kalt *et al.* 1999; Rosenau *et al.* 2001). Both the NMMO decomposition and regeneration reactions are considered in the model.

The simulation model is controlled using design constraints that can be met with certain set of design variable values. The design constraints fix the key process design parameters to targeted values. The simulator automatically solves the steady-state to fulfil the design constraints by varying the design variable values. The simulation software uses the SQP-solver (Sequential Quadratic Programming) to find the solution to the complex numerical problem. The constraints and variables are described in Table 4 for the Base-case.

In addition, several other model constraints (functions describing correlations between model parameters) are used. These are used for fixing other process design parameter values in cases where direct correlation exists (*e.g.*, values given as %-value on dry pulp or fibre). These two sets of constraints enable flexible use of the model in sensitivity and scenario analyses.

Table 4. Design Constraints and Variables

Controlling Target	Design Constraint	Target Value for Constraint	Design Variables
Process capacity	Amount of produced fibre	50 000 t/a	Raw material feed to process
Fibre drying process and final dryness	Fibre dry content	88.9%	Drying air recirculation rate, Dryer air flow
	Dryer exhaust moisture content	100 g/m^3 air	
Fibre spinning and washing	Fibre NMMO content	0.5%	Washer shower flow, Fresh water flow to washing, Cooling water flow
	Spin bath NMMO content	20%	
	Spin bath temperature	20 ºC	
Dope conditioning	Dope water content	12.25%	Steam and NMMO flows to dissolution
	Dope cellulose content	12.5%	
NMMO recovery	Recycled NMMO water content	14%	Evaporator steam flow, NMMO degradation rate
	Total NMMO recovery rate	99.7%	

Thermodynamic equilibrium modelling

Several thermodynamic models for describing the equilibrium state of liquid and vapor phase systems exist. In the process conditions of NMMO-Lyocell production, the liquid phase NMMO/H_2O system can be described as a non-ideal solution, predominantly because of molecular associations (interactions) between the compounds. The vapor phase, on the other hand, can be assumed to behave as an ideal gas due to relatively low temperatures and water being the dominant compounds in vapor phase. To model the phase equilibria of such systems, activity coefficient -based methods and equation of states are useful (Mane and Shinde 2012).

In this work, the UNIFAC group contribution method was applied (Fredenslund *et al.* 1975, 1991). For fitting the group contribution parameters of the UNIFAC model, experimental VLE data for the NMMO/H_2O system are needed. However, these data are not publicly available, and an expert opinion on the boiling point elevation of NMMO/H_2O system was used instead as input data for deriving activity coefficients. For comparison, ideal thermodynamics would yield boiling point elevation of 18.5 °C for 86% NMMO/H_2O system compared to the expert opinion of 45 °C.

NMMO/H_2O/cellulose system (dope) is an even more complex system to model. The share of pulp-based organic compounds (cellulose, hemicellulose, lignin) in dope is 12.5 wt%. Phase diagrams of the ternary system NMMO/H_2O/cellulose exist (Eckelt *et al.* 2009); however, they cover only solid/liquid equilibria. In this work, it was assumed that cellulose and other model compounds in solid and liquid phase do not influence the activity coefficients between water and NMMO, and that there is no activity between cellulose and other model compounds and NMMO and water. Cellulose and other model compounds are considered using the simulation software's routines for ideal systems. Additionally, a scenario using simpler thermodynamic model was evaluated.

Washing modelling

Limited amount of performance data for washing Lyocell fibre is available in the public domain. On one hand, the model specification used in this work fully defines the inputs and outputs of the washing block: fixed NMMO content in the washed fibre after the counter-current washing and fixed NMMO content in the spinning bath can be met with certain fresh and recycled water flows. Such mass balance is possible to solve analytically. However, when the recycled water composition changes, as is the case in the considered scenarios, more detailed parameterization of washing is needed.

The Lyocell fibre washing system design assumed for the modelling follows the one described above and in literature (Zauner 2017). The same design of the washing block is used for all evaluated scenarios. The five washing stages are also assumed to behave identically. One convenient way to parameterize such washing sequence is to use three parameters for each washing step, as illustrated in Fig. 2. The three model parameters used to adjust the washing efficiency are i) dry content of the fibre exiting each washing stage, ii) shower wash water flowrate to each washing stage, and iii) K-value for NMMO in each washing stage. The K-value for NMMO (sorption indicator) is specified as mass fraction of NMMO in water phase in the outlet fibre stream per mass fraction of NMMO in water phase in the filtrate. K-value above 1 means that NMMO has sorption tendency to the fibres.

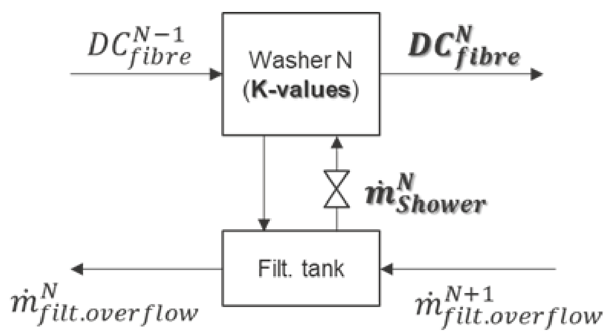

Fig. 2. Illustration of one washing stage in the washing model. The model parameters used to adjust the washing efficiency are highlighted. N = washing stage index, DC = dry content, $\dot{m}$ = mass flow, filt. = filtrate.

In addition to these three washing unit parameters, the NMMO content of the fibre stream entering the first washing stage after the spinning influences the overall washing performance. Fibre NMMO content is dependent on the mass transfer of NMMO from fibre to the bath, which is driven by the bath NMMO concentration. The bath volume is assumed to be large in comparison to the fibre stream flowing through it, and the NMMO concentration is assumed to be constant in the bath. With the modelling level of detail suited for this work, concentration profiles inside unit operations (*i.e.* fibre inside the spinning bath) are not commonly considered. Instead, overall constant conditions are used to calculate output stream compositions in similar way as for washing (see above). Moreover, volumes (hold-ups) are not explicitly modelled in steady-state simulation. The effect of volume, or better described in this case the mass fraction of fibre (bath consistency in Table 1) in the bath at any given time, can be adjusted in the model using circulation of the bath content. The mass transfer in the spinning is assumed to behave similarly as in washing and therefore the same K-value is used.

To fix these four model parameters, sensitivity analysis was conducted for the Base-case scenario. The initial parameter values and the ranges used in the sensitivity analysis are shown in Table 5.

Table 5. Initial Washing Parameterization and Ranges Used in the Sensitivity Analysis of Base-case Scenario

Parameter	Initial Value	Sensitivity Analysis Range	Note
$\mathrm{DC}_{\mathrm{fiber}}^{\mathrm{N}}$	50%	40% ... 60%	Same value for fibre exiting the spinning bath and each washing stage
$\dot{\mathrm{m}}_{\mathrm{Shower}}^{\mathrm{N}}$	$4.1\dot{m}_{fiber}^{N-1}$	2.7 … 6.8	Same value for each washing stage; Initial value solved using NMMO K-value of 2
K-value for NMMO	2	0.5 … 3	All other liquid phase model compounds follow water (K-value is 1)
Fibre mass fraction in spinning bath	0.5%	0.25% ... 1%	

Electricity consumption modelling

Estimation of electricity consumption without detailed process configuration, properties of process stream, and specific electricity demand of process equipment is challenging. Commonly, in early-stage conceptual studies, published electricity consumption values of the target process or similar process design contexts are adopted. More detailed analysis is however needed in this work to account for possible differences in the electricity demand in the considered scenarios.

Table 6. Assumptions for Electricity Consumption of Key Production Processes and Support Processes, Adopted from Pulp and Paper and Biobased Industrial Contexts. Weight Unit Refers to Input or Output of the Process Unit/Department

Key Production Processes	Value	Unit	Notes
Pulper [a, b]	30	kWh/t dry	Range 10 to 40 kWh/t
Press [b]	15	kWh/t dry	Range 10 to 15 kWh/t
Mixer [a]	10	kWh/t dry	Range 10 to 15 kWh/t
Dissolving [c]	40	kWh/t evaporated	Single-stage evaporator
Fibre spinning (*e.g.* pumping through dope filters (up-to 180 bar pressure [d]), circulation, bath cooling)	15	kWh/t dope	Assumption
Washing and post-treatment [b]	30	kWh/t	Range 5 to 60 kWh/t
Drying [b]	120	kWh/t dry	Range 60 to 150 kWh/t
Flotation and filtering [e, c]	5	kWh/t permeate	
Ion-exchange	2.5	kWh/t permeate	Assumption
Evaporation [c, f]	4	kWh/t evaporated	Range 4 to 5 kWh/t evaporated in multi-stage evaporator
Other processes (*e.g.* cooling tower, chemical preparation, effluent and water management, miscellaneous consumers and losses)	10	% of total	Assumption
Support processes [g, h] (*e.g.* lighting, HVAC, administration related, compressed air)	30	% of total	Range 28% to 43% for biobased industries

[a] Mandl 2016, [b] Suhr, Michael *et al.* 2015, [c] Hermann and Patel 2007, [d] White 2001, [e] European Commission 2009, [f] Pulp and Paper Research Institute of Canada 2008, [g] Andersson *et al.* 2018, [h] Thollander *et al.* 2015

The modelling of electricity consumption in this work is based on specific electricity consumption of production processes and support processes. The assumptions are listed in Table 6.

Economic Analysis

The economic performance metric selected for this study is production costs of Lyocell fibre, measured in EUR/t fibre (88.9% dry content). This metric can clearly show the cost implications of technical changes in the design and design assumptions. On the other hand, it is simple enough to enable tracking of the real cause of the change. For instance, compared to commonly used investment project profitability metrics, such as internal rate of return (IRR) or net present value (NPV), changes due to the technical assumptions are not hidden behind several layers of assumptions. Also, the economic analysis of this work is meant for comparing alternative concepts, not to support plant investment decision-making processes.

Economic analysis considers both variable and fixed production costs. Fixed costs, even though potentially constant in the scenarios, were included to better account for relative importance of different variables. Sensitivity analyses of this study also cover fixed cost parameters.

Variable production costs

The variable production costs are evaluated by multiplying the input and output balance values by unit prices shown in Table 7.

Table 7. Unit Prices of Inputs and Outputs

	Value	Unit
Dissolving pulp [a] (discount [b])	900.0 (22%)	EUR/t
Electricity [c]	115	EUR/MWh
Steam LP [d]	20	EUR/MWh
Water, process [e]	2.6	EUR/m3
Water, raw (cooling) [d]	0.02	EUR/m3
NMMO (50%) [f]	4	EUR/kg
Finisher [g]	2.4	EUR/kg
HCl (32%) [h]	0.2	EUR/kg
NaOH (50%) [i]	0.4	EUR/kg
H_2O_2 (50%) [j]	0.4	EUR/kg
Propyl gallate [k]	17.2	EUR/kg
Hydroxylamine [l]	4	EUR/kg
Wastewater [d]	1	EUR/m3
Logistics [m]	7.9	% on sales [n]

[a] Research and Markets 2019, [b] Natural Resources Canada 2014, [c] Eurostat 2021a, [d] Hytönen and Leppävuori 2014, [e] Water News Europe 2021, [f] Shafiei *et al.* 2011, [g] Zauba 2022, [h] DIYTrade International. 2022a, [i] Infinity Galaxy 2022, [j] DIYTrade International. 2022b, [k] Molbase 2022, [l] WITS World Integrated Trade Solutions 2022, [m] Mak 2018, [n] Average textile fibre price of 2500 EUR/t used for sales value estimation; Monica Jiang 2022

Fixed production costs

The fixed production costs were estimated using commonly used approaches and definitions (Towler and Sinnott 2008). The evaluated cost categories included annualized capital costs, personnel related costs, maintenance costs, and other fixed production costs.

Annualized capital costs are estimated as fixed capital investment (FCI) annualized over 20 years at a 5.18% discount rate (Aswath Damodaran 2022). The fixed capital investment was estimated using Taylor's significant process step -based method described in (Taylor 1977) and shown in Eq. 1.

$$C_{ISBL} = 0.042\, Q^{0.39} \sum_{i=1}^{N} 1.3^{S_i} \quad (1)$$

where C_{ISBL} is the Inside Battery Limits costs (M£, 1977, UK), Q the plant capacity (kt/a), i the index for significant process steps, N the number of significant process steps and S_i the complexity score of significant process step i. The obtained C_{ISBL} was further location, currency and time adjusted to year 2021 western European project using location factors (Towler and Sinnott 2008), online currency exchange data and The Chemical Engineering Plant Cost Index (CEPCI) (Vatavuk 2002; Charles Maxwell 2020).

The Inside Battery Limits (ISBL) cost estimate obtained with Eq. 1 was converted to fixed capital investment and total capital investment (TCI, in MEUR) estimates using Eq. 2 and factors presented in Table 8.

$$TCI = FCI + C_{WC} = C_{ISBL} + C_{OSBL} + C_{IND} + C_{WC} \quad (2)$$

where C_{WC} is working capital (MEUR), C_{OSBL} is Outside Battery Limits costs (MEUR) and C_{IND} indirect capital costs (MEUR), including engineering costs and contingency charges. Results from using this method were compared to publicly available announced similar project costs that were assumed to represent total capital investment cost values including all items presented in Eq. 2.

Table 8. Total Capital Investment Breakdown – Assumed Most Likely Value for Factors, Cost Basis and Range. Adapted from (Towler and Sinnott 2008)

	Factor	Basis	Range
C_{ISBL}			95% confidence interval: +36% to -26% [a]
C_{OSBL}	40%	C_{ISBL}	10 to 100%, 40% commonly used for initial estimates
C_{IND}	50%	C_{ISBL}+ C_{OSBL}	Engineering costs between 10% and 30%, contingency charges between 10% and 50%; the case study process is a large-scale process leading to relatively lower engineering costs
C_{WC}	10%	FCI	10 to 20% commonly used
[a] (Taylor 1977)			

Personnel costs are calculated based on factors explained in Towler and Sinnott (2008): Average amount of operators per shift position is 4.8, and supervision is 25% of operating labor. Several shift positions are needed in every process department (Fig. 1). Additionally, operators are needed in handling incoming dissolving pulp, in baling and packaging of the product, in product storage, and in the chemical storage area. In the Base-case scenario the calculated number of operators and supervision personnel are 159 and 40 respectively (total 199). In the Simplified recovery scenario, fewer operators are needed in NMMO recovery, leading to total of 187 persons, whereas in Low bath NMMO content -scenario more operators are assumed to be needed in recovery, and the total personnel amount is 205. The average hourly labor cost of 29.1 EUR/hour (2021) from Eurostat (Eurostat 2021b) was used to convert the total personnel amount to personnel costs.

Fixed cost factors are explained in Table 9. Sales and marketing costs are assumed to be included in the general plant overhead. No license or royalty payments are assumed in this work.

Table 9. Factors for Calculating Fixed Costs (Towler and Sinnott 2008)

Factors	Value	Basis
Annual maintenance costs	4%	C_{ISBL}
Other fixed production costs (incl. property taxes and insurances, rent of land and environmental charges)	3%	C_{ISBL} + C_{OSBL}
general plant overhead	65%	Labor + maintenance cost

RESULTS AND DISCUSSION

Process Analysis

Mass and energy balances

The flowsheet of the simulation model for the Base-case scenario is shown in Fig. 3, and the input-output mass and energy balances for considered scenarios in Table 10. The flowsheets of the other scenarios are identical with the exception of the Simplified recovery scenario: the three last evaporation stages are bypassed to simulate 3-stage evaporation system and the evaporation vents are led after condensing to wastewater treatment rather than recirculated back to evaporation for NMMO recovery. Also, in the Simplified recovery scenario, NMMO regeneration is bypassed and input stream S6 has zero flow.

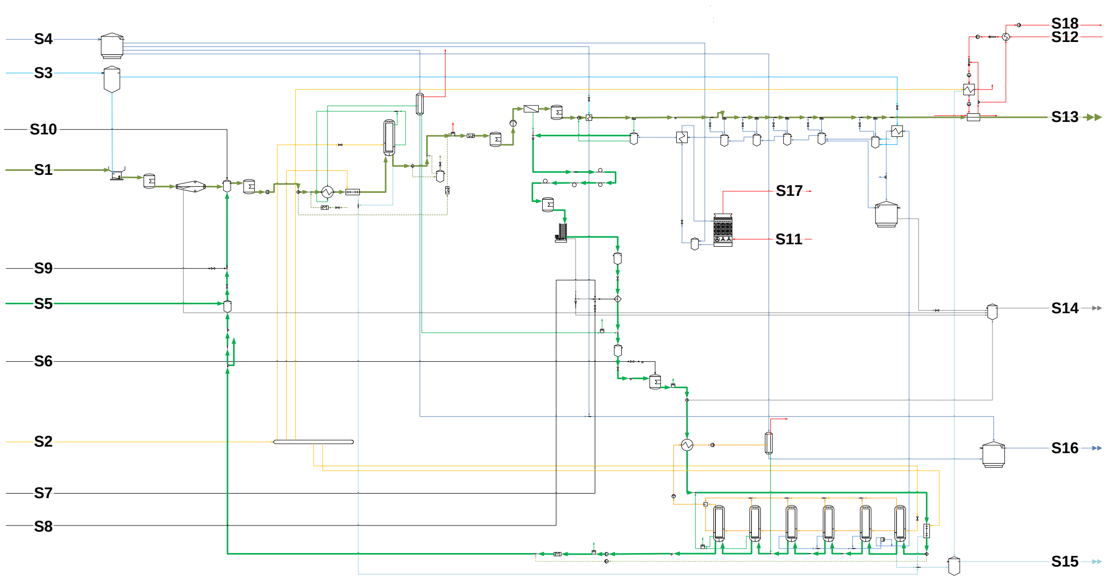

Fig. 3. Base-case -scenario simulation model flowsheet. Line colors: Olive green = fibre, green = solvent cycle, ice blue = cooling water, yellow = steam, orange = vents, black = chemicals, light turquoise = steam condensate, light blue = fresh water, red = air, grey = wastewater. All input and output streams without flowrate have zero flow.

The main differences in the mass and energy balances between the scenarios are illustrated in Table 11 and Fig. 4.

The decreased NMMO recovery rate in the Simplified recovery scenario is a result of the scenario definition: NMMO regeneration system was not included as part of the design and the evaporation vents were led after condensing to wastewater treatment compared to other scenarios where NMMO regeneration was part of the design, and the evaporation vents were recirculated back to evaporation to minimize NMMO losses in the process.

Table 10. Mass and Energy Balance of Considered Scenarios *

	Stream		Base-case	Simplified Recovery	Ideal Thermodynamics	Low Bath NMMO Content	Unit
IN	Dissolving pulp	S1	136	136	136	136	t/d
	Electricity		190	273	192	214	MWh/d
	Steam, LP	S2	1765	2862	1752	2341	t/d
	Water, process	S3	2659	3535	4506	2805	m3/d
	Water, raw (cooling)	S4	36011	149335	29408	45654	m3/d
	NMMO (50%)	S5	4.70	25.35	38.33	4.70	t/d
	Finisher		0.12	0.12	0.12	0.12	t/d
	H_2O_2 (50%)	S6	2.9	0.0	2.9	3.0	t/d
	HCl (32%)	S7	12.2	12.2	12.3	16.2	t/d
	NaOH (50%)	S8	8.0	8.0	8.0	10.6	t/d
	Propyl gallate	S9	0.24	0.24	0.24	0.24	t/d
	Hydroxylamine	S10	0.12	0.12	0.12	0.12	t/d
	Cooling tower air	S11	1525	1525	1525	1525	m3/d
	Dryer air	S12	1055	1055	1055	1055	m3/d
OUT	Textile fibre	S13	137	137	137	137	t/d
	Wastewater	S14	2555	3358	4436	2699	m3/d
	Steam condensate	S15	1758	2848	1745	2332	m3/d
	Water, cooling	S16	35771	149187	29220	45310	m3/d
	Cooling tower air	S17	1765	1765	1765	1765	m3/d
	Dryer air	S18	1161	1161	1161	1161	m3/d

* **Note:** Stream numbers are indicated in Fig. 3; Electricity and finisher are not considered in simulation model; Instead, they are evaluated separately.

Table 11. Overall Differences between Considered Scenarios as Unit Consumptions

	Unit	Base-case	Simplified Recovery	Ideal Thermodynamics	Low Bath NMMO Content
NMMO recovery rate	%	99.7%	98.9%	97.6%	99.7%
Fresh water amount	m3/t dry fibre	21,8	29,0	37,0	23,0
Wastewater amount	m3/t dry fibre	21,0	27,6	36,4	22,2
Cooling water amount	m3/t dry fibre	296	1226	242	375
Steam amount	t/t dry fibre	14,5	23,5	14,4	19,2
Electricity	MWh/t dry fibre	1,56	2,24	1,58	1,76
H_2O_2	kg/t dry fibre	23,8	0,0	23,7	24,4

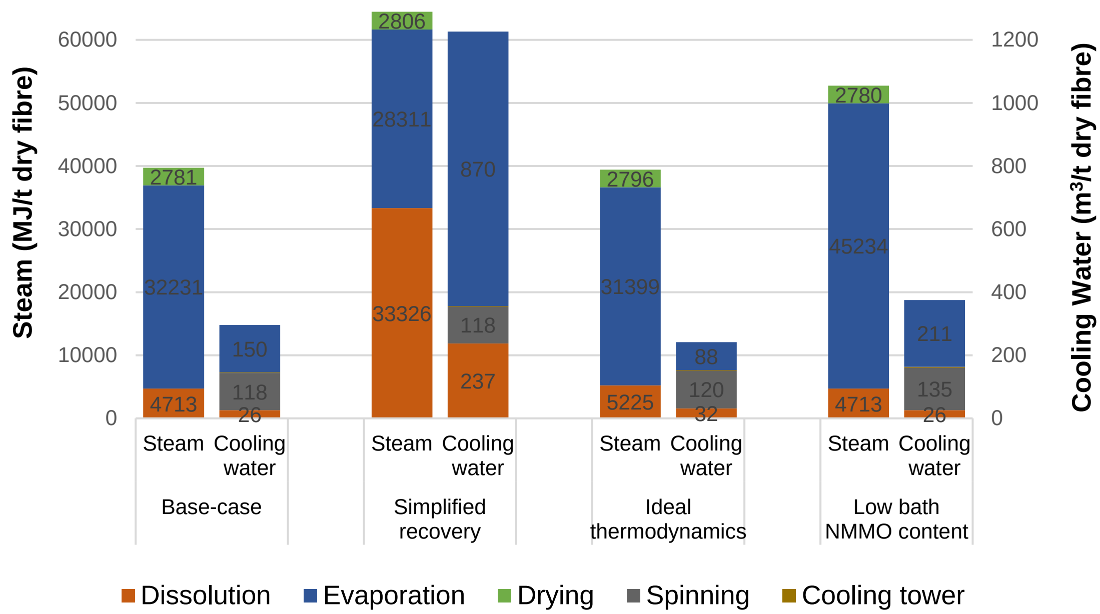

Fig. 4. Breakdown of steam and cooling water amount in considered scenarios

In the Simplified recovery -scenario, the NMMO content after the three-stage evaporation system was only 50%, whereas in other scenarios, it was 86% after the six-stage evaporation system. It was found on this basis that there was less water from evaporation available for fibre washing. The difference was then met by increasing the fresh water use.

In the Ideal thermodynamics scenario, on the other hand, the use of the ideal thermodynamic model results in major NMMO losses because it allows the NMMO model compound to vaporize already at low NMMO content. In the evaporation model, the evaporated water (and other volatile compounds) from first three stages is condensed in the next evaporation stage (*i.e.* evaporated water from 1st stage is used as heat source in the 2nd stage, where it condenses) and recycled as condensate to be used in fibre washing. To reach targeted fibre NMMO content after washing, the washing waters cannot have too high NMMO content, and as a result, the amount of recycled water needs to be constrained in this scenario to a level that enables the washing. Therefore, more evaporated water is led to wastewater treatment and corresponding amount of fresh water is used in washing. At the same time, the NMMO recovery rate decreases, since more NMMO is lost with the wastewater.

The cooling water demand follows tightly the cooling needs of evaporation vent condenser. In the Simplified recovery scenario, the evaporation vents needs to be cooled down to low temperature to be suitable for wastewater treatment. In other scenarios, the vents are circulated back to evaporation where the temperature is higher and cooling need in the condenser is lower. In addition, in the Simplified recovery scenario, the evaporation in dissolution has noticeably higher evaporation rate because pre-dope contains more water than in other scenarios. This leads to higher cooling need in dissolution vent condenser. In Low bath NMMO content-scenario, the total volume of water to be evaporated in NMMO recovery is about 40% higher which leads to higher cooling demand in the evaporation vent condenser.

The higher steam demand is mainly a result of above-mentioned reasons. In the Simplified recovery scenario more water needs to be evaporated in the dissolution. Because the single-effect dissolution evaporator has lower steam efficiency compared to multi-effect evaporation, more steam is needed. In the Low bath NMMO content scenario, the spinning bath NMMO content is 15% compared to 20% in other scenarios. Correspondingly, the feed to evaporation contains more water that needs to be evaporated and therefore more steam is needed. In the Ideal thermodynamics scenario, on the other hand, less steam is needed (and correspondingly cooling water). This results from the design decisions: the evaporation process configuration and the temperature of the concentrated NMMO are kept the same between the scenarios with six-stage evaporation. Fixing the temperature in the Ideal thermodynamics scenario is done by increasing the pressure levels of the evaporation stages. Almost the same amount of water and NMMO are evaporated in this and the Base-case scenario. However, due to easier vaporization of NMMO in the Ideal thermodynamics scenario, more NMMO is evaporated in first three stages and leave the evaporation, whereas in the Base-case scenario with UNIFAC thermodynamic model, much less NMMO is vaporized in the first three stages. In the last three stages, due to higher pressure needed to remove water from the system, relatively more NMMO is evaporated in the Base-case scenario compared to the Ideal thermodynamics scenario. This also requires more energy, and thus the total energy requirement in the Base-case scenario is somewhat higher.

As defined, in the Simplified recovery scenario there is no NMMO regeneration and therefore there is no need for H_2O_2. A slightly higher need of H_2O_2 in the Low bath NMMO content scenario results from the slightly increased NMMO vaporization in evaporation: a larger amount of water is evaporated, which also strips more NMMO to vents that are led to NMMO regeneration.

It can be seen from these technical concept analysis results that the study design and process concept design are important factors of such work. In this work, the process designs were not optimized for each scenario; instead, the goal was to try to isolate the impacts of one important design decision at a time with fixed design. The NMMO recovery efficiency could potentially be adjusted to 99.7% in all scenarios by modifying the process configurations. Similarly for the other key differences, by modifying the configuration and adding new processing steps could lead to more optimized process concepts.

Washing modelling

To identify washing parameterization, sensitivity analysis was conducted for the Base-case scenario (shown in Fig. 5). In the sensitivity analysis, four parameters affecting the washing efficiency were varied with sensitivity analysis ranges presented in Table 5.

The washing result, *i.e.*, the fibre NMMO content, is very dependent on the shower wash water flowrate and the dry content of fibre between the washing stages, as shown in Fig. 5. Also, K-value indicating the sorption tendency of NMMO on fibres has a notable impact on the final fibre NMMO content. Instead, the fibre mass fraction in the spinning bath seems not to affect the NMMO content of the fibre. Because there are parameters both increasing and decreasing the fibre NMMO content, several sets of parameters could be possible to reach the same target level (0.5% NMMO content of dry fibre, and 20% spinning bath NMMO content). The NMMO content of commercial fibres or the details of washing process are not publicly available information. The selected initial parameter values (Table 5) fulfil the target values and thus were adopted for all evaluated scenarios.

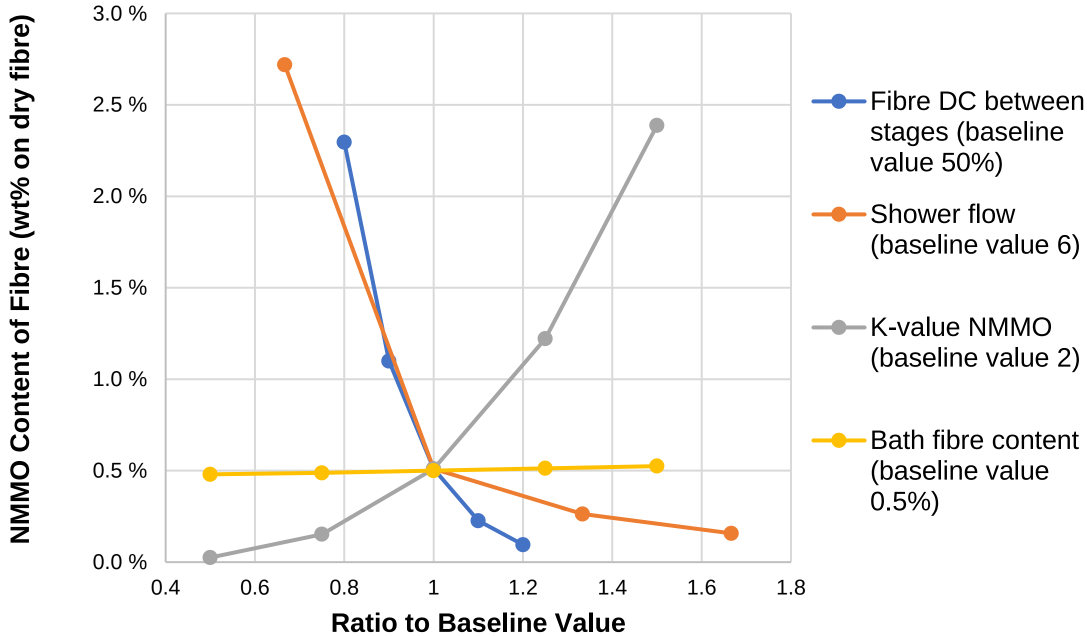

Fig. 5. Sensitivity of fibre NMMO content on washing model parameters in Base-case scenario

Electricity consumption

The annual electricity consumption distribution in the scenarios is illustrated in Fig. 6. Overall, fibre production unit processes and NMMO recovery unit processes consume 30 to 46% and 14 to 30% of electricity respectively. Support and other processes together consume, as defined, 40% of total electricity need.

The main difference between the scenarios comes from the change in the NMMO recovery system. The dissolution process is assumed to have ten times higher specific electricity demand per evaporated water volume compared to multi-stage evaporation process. In the Simplified recovery -scenario, less water is evaporated in the evaporation but more in dissolution. Therefore, the electricity consumption of dissolution is notably higher than in other scenarios.

On the other hand, the evaporation process electricity consumption is much lower than in other scenarios. In Low bath NMMO content -scenario, on the other hand, the volumes processed in recovery cycle increase markedly. That increases, for example, the need for pumping.

In the Ideal thermodynamics scenario, the evaporation system processes larger volume due to the higher evaporation rate of NMMO when using ideal thermodynamic model instead of the activity coefficient -based model used in other scenarios. This does not however notably increase the calculated electricity consumption.

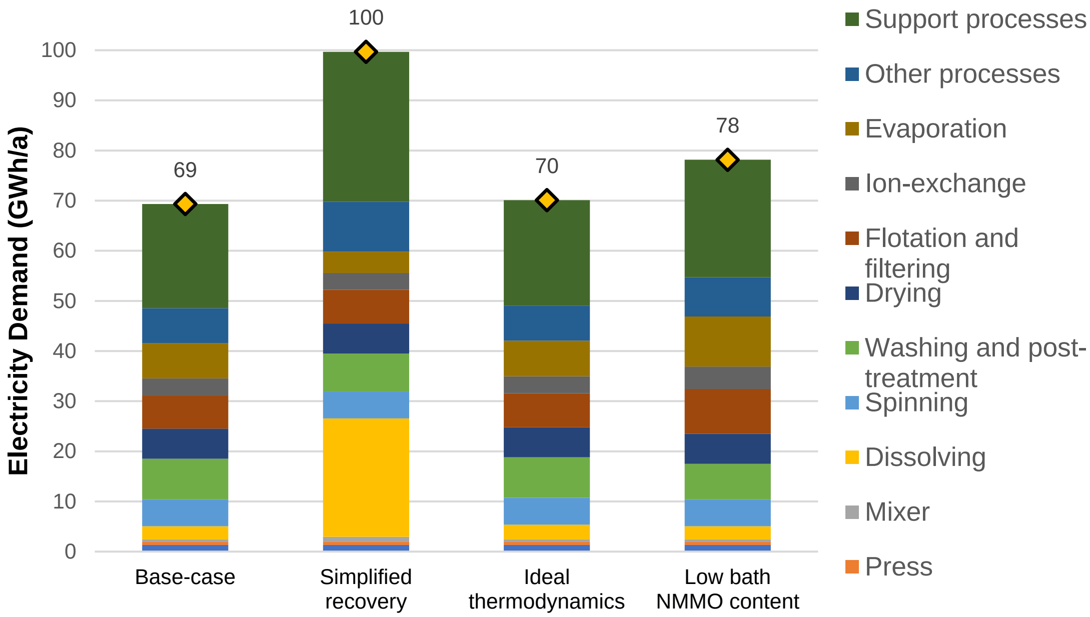

Fig. 6. Calculated annual electricity consumption distribution in analyzed scenarios

Economic Analysis

Capital investment cost estimation

The capital cost estimates for the considered scenarios are shown in Table 12. The ISBL cost estimate is obtained by evaluating the costliness index for 27 separate significant process steps of the processes in each of the scenarios. The scoring of relative throughput was based on the simulated mass and energy balances. Storage time was assumed to be 3 to 4 weeks for dissolving pulp and fibre product, and 5 to 7 weeks for chemicals. All separation processes are assumed to be operated under pressure or vacuum, especially dope filter in very high pressure. All process steps where NMMO is present are expected to require at least stainless-steel construction material. Dissolution and spent NMMO evaporation steps are film evaporation type steps. All other scoring criteria are assumed be equal to zero, *e.g.* no multi-streaming is assumed (single line process assumed).

Resulting from the scenario definition, in Simplified recovery -scenario, there are two significant process steps less than in the other scenarios. This together with lower flowrates in evaporation effectively lower the costliness index for the scenario, even though the dissolution and NMMO storage are larger, and in turn increase the costliness index.

When comparing the scenarios, it can be seen that the capital cost investment estimates differ only slightly between the scenarios, and the differences are well within the 95% confidence limits of the method, which is reported by Taylor to be -26%...+36% (Taylor 1977).

When comparing the obtained values to publicly announced investment cost values, a few underlying aspects need to be accounted for in addition to location and time corrections. These include at least the ratio between ISBL costs and announced investment cost values, possible multi-streaming in the plant, and learning curve. The CISBL/TCI ratio might differ from the one assumed in this work due to for example the type of investment (capacity increase in existing site *vs*. green field plant). Multi-streaming can be a design decision to partially de-risk *e.g.*, market demand related issues (division of the production line into several parallel lines). In addition, the learning curve between first-of-a-kind plant and the N^{th} plant can lead to cost decreases over time. These factors are not published with the total investment values, nor are the cost items included in the total values. Estimating capital costs using Eqs. 1 and 2 assume N^{th} plant design and that common chemical industry factors are right for this design context correspondingly.

Table 12. Capital Cost Investment Estimates for the Scenarios

MEUR	Base-case	Simplified Recovery	Ideal Thermodynamics	Low Bath NMMO Content
C_{ISBL}	155	150	154	158
C_{OSBL}	62	60	62	63
C_{IND}	109	105	108	111
FCI	326	314	324	332
C_{WC}	33	31	32	33
TCI	359	346	357	366

A few capital investment cost values of NMMO Lyocell plants have been announced in recent years: Kara Holding has announced in 2020 total capital costs of 400 MEUR for a plant with 80 kt/a production (E-Textile Magazine 2019), Baoding Swan Fiber Co. Ltd. has announced in 2016 about 310 MEUR (0.136 EUR/Yuan) investment for a 60 kt/a plant (Baoding Swan 2019), and Lenzing AG has announced in 2022 a capital cost of 400 MEUR for 100 kt/a plant (Fibre2Fashion 2022). The value obtained for the Base-case -scenario with 50 kt/a production is well in line with those values reported, considering that time corrected values for publicly announced investment costs are somewhat higher in the study basis year 2021.

Production cost estimation

The production costs in the considered scenarios are illustrated in Fig. 7. The total production costs in the analyzed scenarios range between 2810 and 3835 EUR/t fibre.

The variable costs of production range between 55% and 67% of total production costs; correspondingly the remainder, fixed costs of production, range between 45% and 33%. The difference in the variable costs between the scenarios is mainly due to NMMO makeup need, which derives from the NMMO recovery rate difference. It can be observed that the decrease of NMMO recovery rate from 99.7% to 98.9% (from Base-case to Simplified recovery -scenario) increases the makeup NMMO costs by 600 EUR/t. The change from efficient to less efficient NMMO recovery system (from Base-case to Simplified recovery -scenario) consumes more electricity and steam. This can be seen as an additional increase in production costs by about 190 EUR/t. Thus, the costs are very sensitive to NMMO recovery efficiency.

In the Process Analysis chapter, the impact of washing model parameterization on Lyocell fibre NMMO content was discussed. It was shown that, for example, by relatively small change in the fibre dry content after all washing stages from baseline value of 50% to 40%, the NMMO content of the fibre changes from 0.5% to 2.3% on dry fibre when all other washing parameters are kept constant. An NMMO content of 0.5% on dry fibre corresponds to about 25% of the total NMMO losses. Assuming that all other NMMO losses in the process are the same, increasing the fibre NMMO content to 2.3% would nearly double the NMMO makeup need and decrease the NMMO recovery rate from

99.7% to 99.4%. Combining this to the Simplified recovery scenario results indicates that washing can potentially have an influence on the costs. However, there is not enough published data available on the washing of Lyocell fibre to be able to judge whether such high NMMO losses with the fibre are a realistic scenario. Moreover, based on the assumptions and modelling work in this study, NMMO decomposition and losses in recovery cycle take up the remaining 75% of the total NMMO losses and are thus a larger contributor to makeup NMMO costs and overall economics than the washing.

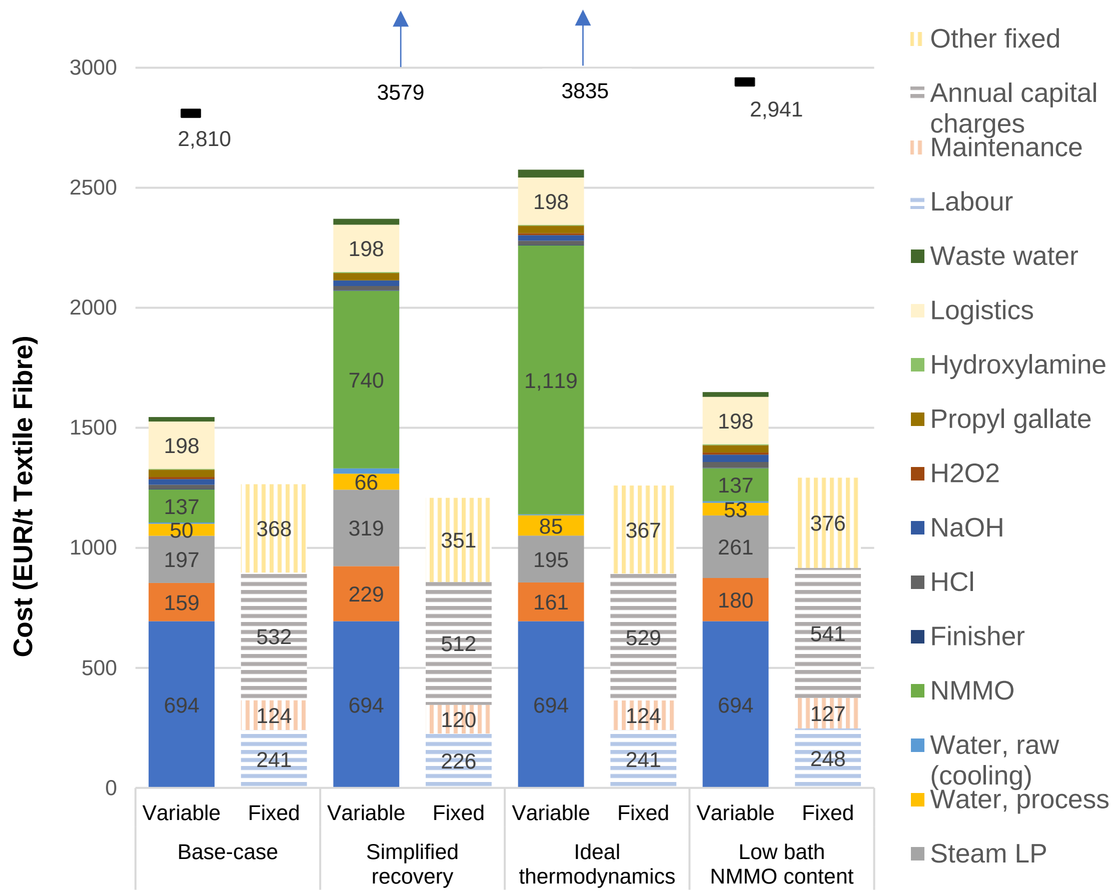

Fig. 7. Variable (solid columns) and fixed (striped columns) production cost breakdown for considered scenarios. Total costs of Simplified recovery and Ideal thermodynamics -scenarios are outside the chart scale.

All other production cost items are very similar between the scenarios. The annual capital charges and capital costs estimate-based fixed cost items differ by 2 to 5% and the labor cost by 3 to 6% from the Base-case -scenario values.

Sensitivity analysis

Based on the production cost breakdown presented in Fig. 7, the key variable cost items in all scenarios are dissolving pulp, electricity, LP steam, NMMO, and logistics. In addition, all fixed cost items are prominent. The sensitivity of the total production costs on varying all these items by + 25% from their baseline value in Base-case and Simplified recovery -scenarios are shown in Fig. 8 a) and b) respectively.

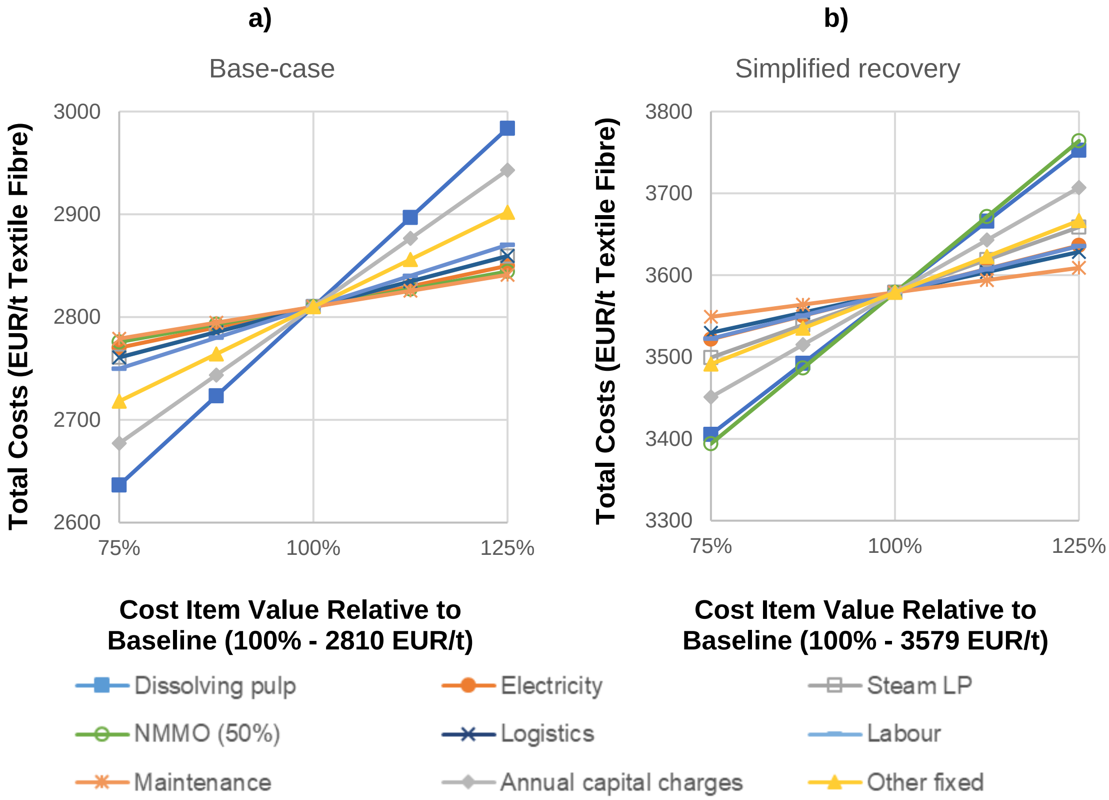

Fig. 8. Sensitivity of Total costs (EUR/t) on key cost items in a) Base-case and b) Simplified Recovery -scenarios. Note different y-axis scale.

The changes in the cost item values can be considered to result from several factors: uncertainty in unit prices, uncertainty in the engineering work results (design decisions, model parameters, mathematical models), or a combination of those. The uncertainty in the process design is evident as detailed process configurations and parameterizations for the scenarios is not available in public domain. However, the decisions made on the process design and parameterization is verified maximally with public domain understanding and expert opinions. The mathematical models, used in process simulation model and cost model, are robust and tested as commercial tools and proven methods are used. The mathematical models used for thermodynamics and washing were separately studied and discussed. Other model parameters and unit prices were taken from public sources. Their uncertainty analysis was not in focus of this work, instead, this sensitivity analysis was aimed at studying their impacts.

Figure 8 a) shows that two of the key cost items have the biggest cost reduction potential: reduction of 25% in annual capital charge or in dissolving pulp price can decrease the total production costs by 4.7% and 6.2% respectively. Decrease in the other cost items results in smaller cost reduction. In the Simplified recovery scenario (Fig. 8 b), also NMMO cost has large cost reduction potential. Because factorial method was adopted in this study for fixed cost calculation, the following aspects need to be remembered: Total capital investment estimate influences the annual capital charges, maintenance costs and other fixed costs as defined in Table 9, and labor costs influence the other fixed costs.

CONCLUSIONS

1. The fibre production cost in the hypothetical case study (Base-case) is 2810 EUR/t with NMMO makeup cost contribution of 5%. When NMMO recovery rate is decreased from 99.7% to 98.9%, the NMMO makeup cost is 5.4 times higher. High recovery rate can be reached with efficient fibre washing with clean washing waters, and with capturing all NMMO and its degradation products from vents and waters. However, the production costs are more sensitive to capital charge and dissolving pulp cost.
2. In the Base-case scenario the two evaporation unit operations considered account for 93%, 60%, and 14% of all steam, cooling water, and electricity needs, respectively, of the plant. These translate to about 7% of total production costs. Additionally, about 18% of ISBL (and other costs dependent on capital costs) is related to evaporation. Therefore, evaporation is one of the key unit operations when designing NMMO-Lyocell process. One process design parameter influencing the total costs attributable to evaporation is the bath NMMO content – 5% lower NMMO content can increase these costs by 130 EUR/t.
3. The impact of washing and water use on the production costs is minimal. Fresh water cost is less than 2% of total production costs. Furthermore, 86% of fresh water consumption is due to repulping of dissolving pulp, and majority of that water is pressed out and sent to wastewater treatment before dissolution. Thus, even though critical for NMMO recovery rate and fibre purity, washing is not a critical cost item.
4. The results show that needed NMMO recovery efficiency for economic operation cannot be reached in the considered process design using the ideal thermodynamic model. The NMMO model compound evaporates more easily compared to the group contribution based thermodynamic model. Recapturing NMMO from evaporation condensates would require additional processing. Moreover, evaporation condensates with higher NMMO content cannot be used in washing without suitable dilution with fresh water. This leads to higher wastewater generation and fresh water need. Overall, 36% higher production costs resulted from using the ideal thermodynamic model.

ACKNOWLEDGEMENTS

Mr. Andreas Reipsar is acknowledged for his contribution in establishing the first version of the process simulation model as part of his Thesis work. Dr. Frank-Günter Niemz is acknowledged for the valuable inputs and discussions related to the process design and parameterization. This study has received funding from the Bio-Based Industries Joint Undertaking under the European Union’s Horizon 2020 research and innovation programme under grant agreement No. 837527.

REFERENCES CITED

Andersson, E., Arfwidsson, O., and Thollander, P. (2018). “Benchmarking energy performance of industrial small and medium-sized enterprises using an energy

efficiency index: Results based on an energy audit policy program," *Journal of Cleaner Production* 182, 883-895. DOI: 10.1016/j.jclepro.2018.02.027
Aswath Damodaran (2022). "Damodaran Online: Home Page for Aswath Damodaran," (https://pages.stern.nyu.edu/~adamodar/), accessed October 18, 2022.
Baoding Swan (2019). "How Can Baoding Swan Up In The Face Of Difficulties? The Answer To Transformation And Upgrading Is Given," (https://www.sjfzxm.com/global/en/553570.html), accessed August 8, 2022.
Bialik, M., Jensen, A., Kotilainen, O., Kulander, I., and Lopes, M. (2020). "Design, optimization and modelling of a chemical recovery system for wet spinning of cellulose in sodium carbonate solutions," *Cellulose* 27(15), 8681-8693. DOI: 10.1007/s10570-020-03394-1
Biganska, O., and Navard, P. (2003). "Phase diagram of a cellulose solvent: N-methylmorpholine-N-oxide-water mixtures," *Polymer* 44(4), 1035-1039. DOI: 10.1016/S0032-3861(02)00902-3
Biganska, O., and Navard, P. (2004). "Dissolution, crystallisation and regeneration of cellulose in N-methylmorpholine N-oxyde," *Proceedings of MACRO 2004 International Conference on Polymers for Advanced Technologies*, Thiruvananthapuram, India.
Bouwman, M. H. (2008). *Multiphase Simulations of a Lyocell Process*, PhD Dissertation, Montanuniversität Leoben, Leoben, Austria.
Christensen, P., and Dysert, L. R. (2005). "18R-97: Cost Estimate Classification System - As Applied in Engineering, Procurement, and Construction for the Process Industries," AACE International Recommended Practice.
DIYTrade International. (2022a). "Hydrochloric acid," (https://www.diytrade.com/china/pd/20406875/http%3A%2F%2Fwww.diytrade.com%2Fchina%2Fpd%2F20406875%2Fhydrochloric_acid.html), accessed July 10, 2022.
DIYTrade International. (2022b). "50% hydrogen peroxide," (https://www.diytrade.com/china/pd/11666151/http%3A%2F%2Fwww.diytrade.com%2Fchina%2Fpd%2F11666151%2F50_hydrogen_peroxide.html.), accessed July 12, 2022.
Eckelt, J., Eich, T., Röder, T., Rüf, H., Sixta, H., and Wolf, B. A. (2009). "Phase diagram of the ternary system NMMO/water/cellulose," *Cellulose* 16(3), 373-379. DOI: 10.1007/s10570-009-9276-2
Eckelt, J., and Wolf, B. A. (2008). "Thermodynamic interaction parameters for the system water/NMMO hydrate," *J. Phys. Chem. B* 112(11), 3397-3401. DOI: 10.1021/jp710869e
E-Textile Magazine (2019). "Kara Holding to Manufacture Lyocell Fiber with a 400 Million Euro Investment," (https://www.etextilemagazine.com/en/kara-holding-to-manufacture-lyocell-fiber-with-a-400-million-euro-investment.html), accessed October 10, 2022.
European Commission (2009). *Reference Document on Best Available Techniques for Energy Efficiency*. (ENE). Publications Office, (https://eippcb.jrc.ec.europa.eu/reference)
Eurostat (2021a). "Electricity price statistics," (https://ec.europa.eu/eurostat/statistics-explained/index.php?title=Electricity_price_statistics), accessed October 2, 2022.
Eurostat (2021b). "Hourly labor costs," (https://ec.europa.eu/eurostat/statistics-explained/index.php?title=Hourly_labor_costs), accessed August 17, 2022.

Fibre2Fashion (2022). “Lenzing opens world’s largest lyocell plant in Thailand,” (http://www.fibre2fashion.com/news/textile-news/lenzing-opens-world-s-largest-lyocell-plant-in-thailand--279271-newsdetails.htm.), accessed October 10, 2022.
Fredenslund, A., Hansen, H. K., Rasmussen, P., Schiller, M., and Gmehling, J. (1991). “Vapor-liquid equilibria by UNIFAC group contribution. 5. Revision and extension,” *Ind. Eng. Chem. Res.* 30, 2355-2358. DOI: 10.1021/ie00058a017
Fredenslund, A., Jones, R. L., and Prausnitz, J. M. (1975). “Group-contribution estimation of activity coefficients in nonideal liquid mixtures,” *AIChE J.* 21(6), 1086-1099. DOI: 10.1002/aic.690210607
Golova, L. K., Borodina, O. E., Kuznetsova, L. K., Lyubova, T. A.m and Krylova, T. B. (2000). “The solid-phase MMO process,” *Fibre Chem* 32(4), 243-251. DOI: 10.1007/BF02360716
Guo, Y., Cai, J., Sun, T., Xing, L., Cheng, C., Chi, K., Xu, J., and Li, T. (2021). “The purification process and side reactions in the N-methylmorpholine-N-oxide (NMMO) recovery system,” *Cellulose* 28(12), 7609-7617. DOI: 10.1007/s10570-021-03929-0
Hedlund, A., Theliander, H., and Köhnke, T. (2019). “Mass transport during coagulation of cellulose-ionic liquid solutions in different non-solvents,” *Cellulose* 26(16), 8525-8541. DOI: 10.1007/s10570-019-02649-w
Hermann, B. G., and Patel, M. (2007). “Today’s and tomorrow’s bio-based bulk chemicals from white biotechnology: A techno-economic analysis,” *Appl. Biochem. Biotechnol.* 136 (3), 361-388. DOI: 10.1007/s12010-007-9031-9
Hytönen, E., and Leppävuori, J. (2014). “Future Biorefinery (FuBio) research into process concepts – Early stage process evaluation and screening,” *Proceedings of 5th Nordic Wood Biorefinery Conference NWBC 2014*, Stockholm, Sweden, pp. 62-67.
Hytönen, E., and Stuart, P. (2013). “Techno-economic assessment and risk analysis of biorefinery processes,” in: *Integrated Biorefineries: Design, Analysis, and Optimization*, 1st Ed., CRC Press, Boca Raton, FL, USA, pp. 204-239. DOI: 10.1201/b13048
Infinity Galaxy. (2022). “Caustic Soda Price Today,” (https://infinitygalaxy.org/caustic-soda-price/), accessed October 12, 2022.
Jiang, X., Bai, Y., Chen, X., and Liu, W. (2020). “A review on raw materials, commercial production and properties of lyocell fiber,” *Journal of Bioresources and Bioproducts* 5 (1), 16-25. DOI: 10.1016/j.jobab.2020.03.002
Jiang, M. (2022). “Possible demand shift with narrowing price spread of cotton, lyocell and VSF | CCFGroup,” (https://www.ccfgroup.com/newscenter/newsview.php?Class_ID=D00000&Info_ID=2022062230073), accessed August 12, 2022.
Kalt, W., Eichinger, D., Mangeng, B., and Firgo, H. (1999). “Process for the regeneration of an aqueous process liquid of the amine-oxide process,” US Patent US5904818A.
Lidhure, A., Jadhav, S., Ganvir, V., and Thakre, S. (2019). “Modified lyocell process for producing biopolymer fiber,” *Proceedings of PPS-34*, Kelantan, Malaysia. pp. 030062-1-030062-6
Mak, K. H. (2018). *Logistics Cost Minimization and Inventory Management Decision for Yarn Manufacturers in China*, Master’s Thesis, Massachusetts Institute of Technology, Cambridge, MA.
Makarov, I. S., Golova, L. K., Vinogradov, M. I., Levin, I. S., Shandryuk, G. A., Arkharova, N. A., Golubev, Y. V., Berkovich, A. K., Eremin, T. V., and Obraztsova, E. D. (2020). “The effect of alcohol precipitants on structural and morphological

features and thermal properties of Lyocell fibers," *Fibers* 8 (43). 1-15 DOI: 10.3390/fib8060043
Mandl, J. (2016). *Energy Benchmark System for Mondi BP Austria AG*, Diploma Thesis, University of Leoben, Leoben, Austria
Mane, M. B., and Shinde, S. N. (2012). "Vapor liquid equilibria: A review," *Sci. Revs. Chem. Commun.* 2 (2), 158-171.
Maxwell, C. (2020). "Cost Indices - Towering Skills," (https://www.toweringskills.com/financial-analysis/cost-indices/), accessed October 22, 2022.
Molbase (2022). "Propyl gallate price & availability," (https://www.molbase.com/cas/121-79-9.html.), accessed July 11, 2022.
Natural Resources Canada (2014). "Rising list pulp prices supported by rising discounts | Selective Cuttings | Natural Resources Canada," (https://cfs.nrcan.gc.ca/selective-cuttings/67?wbdisable=true), accessed October 12, 2022.
Oliva, A., Tan, L. C., Papirio, S., Esposito, G., and Lens, P. N. L. (2022). "Use of N-Methylmorpholine N-oxide (NMMO) pretreatment to enhance the bioconversion of lignocellulosic residues to methane," *Biomass Conv. Bioref.* DOI: 10.1007/s13399-022-03173-x
Paccot, C. (1987). *Analyze Exergétique des Usines de Pâte à Papier par Simulation*, PhD Dissertation, Grenoble INPG, Grenoble, Isère, France
Perepelkin, K. E. (2007). "Lyocell fibres based on direct dissolution of cellulose in N-methylmorpholine N-oxide: Development and prospects," *Fibre Chem* 39(2), 163-172. DOI: 10.1007/s10692-007-0032-9
Pulp and Paper Research Institute of Canada (ed.). (2008). *Benchmarking Energy Use in Canadian Pulp and Paper Mills*, Pulp and Paper Research Institute of Canada, Pointe-Claire, Quebec, Canada.
Reid, R. C., Prausnitz, J. M., and Sherwood, T. K. (1977). *The Properties of Gases and Liquids*, McGraw-Hill, New York.
Reipsar, A. (2020). *Modelling of Lyocell Fibre Production and Technical Analysis of Solvent Recovery Concepts*, Master's Thesis, Åbo Akademi, Turku, Finland.
Research and Markets (2019). "Global and China Dissolving Pulp Industry Report, 2019-2025," (https://www.researchandmarkets.com/reports/4845606/global-and-china-dissolving-pulp-industry-report?utm_source=CI&utm_medium=PressRelease&utm_code=bb3tnq&utm_campaign=1304285+-+Global+and+China+Dissolving+Pulp+Industry+Report+2019+Featuring+5+Global+and+9+Chinese+Dissolving+Pulp+Producers&utm_exec=chdo54prd.), accessed April 10, 2022.
Rosenau, T., Potthast, A., Sixta, H., and Kosma, P. (2001). "The chemistry of side reactions and byproduct formation in the system NMMO/cellulose (Lyocell process)," *Progress in Polymer Science* 26(9), 1763-1837. DOI: 10.1016/S0079-6700(01)00023-5
Satari, B., Karimi, K., and Kumar, R. (2019). "Cellulose solvent-based pretreatment for enhanced second-generation biofuel production: A review," *Sustainable Energy Fuels* 3(1), 11-62. DOI: 10.1039/C8SE00287H
Sayyed, A. J., Deshmukh, N. A., and Pinjari, D. V. (2019). "A critical review of manufacturing processes used in regenerated cellulosic fibres: Viscose, cellulose

acetate, cuprammonium, LiCl/DMAc, ionic liquids, and NMMO based lyocell," *Cellulose* 26 (5), 2913-2940. DOI: 10.1007/s10570-019-02318-y
Shafiei, M., Karimi, K., and Taherzadeh, M. J. (2011). "Techno-economical study of ethanol and biogas from spruce wood by NMMO-pretreatment and rapid fermentation and digestion," *Bioresource Technology* 102(17), 7879-7886. DOI: 10.1016/j.biortech.2011.05.071
Shafiei, M., Karimi, K., Zilouei, H., and Taherzadeh, M. J. (2014). "Economic impact of NMMO pretreatment on ethanol and biogas production from pinewood," *BioMed. Research International* 2014, 1-13. DOI: 10.1155/2014/320254
Shao, H., Liu, R., and Hu, X. (2003). "Computer modeling of the Lyocell fibre spinning process," *AUTEX Research Journal* 3 (1), 16-22.
Shen, L., and Patel, M. K. (2010). "Life cycle assessment of man-made cellulose fibres," *Lenzinger Berichte* 88, 1-59.
Sixta, H. (Ed.). (2006). *Handbook of Pulp*, Wiley-VCH Verlag GmbH & Co. KGaA, Weinheim, Germany.
Suhr, M., Klein, G., Kourti, I., Gonzalo, M. R., Santonja, G. G., Roudier, S., and Sancho, L. D. (2015). *Best Available Techniques (BAT) reference document for the production of pulp, paper and board*, Joint Research Centre Institute for Prospective Technological Studies, Seville, Spain.
Taylor, J. H. (1977). "The 'process step scoring' method for making quick capital estimates," *Engineering and Process Economics* 2 (4), 259-267. DOI: 10.1016/0377-841X(77)90004-3
Teghammar, A., Forgács, G., Sárvári Horváth, I., and Taherzadeh, M. J. (2014). "Techno-economic study of NMMO pretreatment and biogas production from forest residues," *Applied Energy* 116, 125-133. DOI: 10.1016/j.apenergy.2013.11.053
Thollander, P., Paramonova, S., Cornelis, E., Kimura, O., Trianni, A., Karlsson, M., Cagno, E., Morales, I., and Jiménez Navarro, J. P. (2015). "International study on energy end-use data among industrial SMEs (small and medium-sized enterprises) and energy end-use efficiency improvement opportunities," *Journal of Cleaner Production* 104, 282-296. DOI: 10.1016/j.jclepro.2015.04.073
Towler, G. P., and Sinnott, R. K. (2008). *Chemical Engineering Design: Principles, Practice and Economics of Plant and Process Design*, Elsevier/Butterworth-Heinemann, Amsterdam.
Tsagkari, M., Couturier, J.-L., Kokossis, A., and Dubois, J.-L. (2016). "Early-stage capital cost estimation of biorefinery processes: A comparative study of heuristic techniques," *ChemSusChem* 9(17) 2284-2297. DOI: 10.1002/cssc.201600309
Vatavuk, W. M. (2002). "Updating the CE Plant Index," *Chemical Engineering* 109.1, 62-70.
Water News Europe (2021). "Water prices compared in 36 EU-cities," (https://www.waternewseurope.com/water-prices-compared-in-36-eu-cities/), accessed October 12, 2022.
Wendler, F., Schulze, T., Ciechanska, D., Wesolowska, E., Wawro, D., Meister, F., Budtova, T., and Liebner, F. (2012). "Cellulose products from solutions: Film, fibres and aerogels," *Proceedings of The European Polysaccharide Network of Excellence (EPNOE)*, Vienna, Austria, pp. 153-185.
White, P. (2001). "Lyocell: The production process and market development," in: *Regenerated Cellulose Fibres*, C. Woodings (ed.), Woodhead Publishing Limited, Cambridge, England.

WITS World Integrated Trade Solutions (2022). "Organic derivatives of hydrazine or of hydroxylamine exports by country," (https://wits.worldbank.org/trade/comtrade/en/country/ALL/year/2021/tradeflow/Exports/partner/WLD/product/292800), accessed November 12, 2022.

Zauba (2022). "Import Data and Price of afilan," (https://www.zauba.com/import-afilan/p-1-hs-code.html%20(Accessed%2025.8.2022)-hs-code.html.), accessed October 12, 2022.

Zauner, P. (2017). *Modelling the Mass Transfer of N-Methylmorpholine N-Oxide during the Washing Process of a Cellulose Filament Bundle*, Master's Thesis, Graz University of Technology, Graz, Austria.

Article submitted: March 13, 2023; Peer review completed: June 17, 2023; Revised version received and accepted: July 12, 2023; Published: July 28, 2023.
DOI: 10.15376/biores.18.3.6384-6411